

The Stochastic Spectral Dynamics of Bending and Tumbling

Chris H. Wiggins,^{1,2,5} Alberto Montesi,^{3,4,5} Matteo Pasquali^{3,4,5}

¹*Department of Applied Physics and Applied Mathematics and*

²*Center for Computational Biology and Bioinformatics
Columbia University, New York NY 10027;*

³*Department of Chemical Engineering and*

⁴*Center for Nanoscale Science and Technology
Rice University, Houston TX 77005;*

⁵*The Kavli Institute for Theoretical Physics,
Santa Barbara CA 93106*

(Dated: October 24, 2018)

Traditional models of wormlike chains in shear flows at finite temperature approximate the equation of motion via finite difference discretization (bead and rod models). We introduce here a new method based on a spectral representation in terms of the natural eigenfunctions. This formulation separates tumbling and bending dynamics, clearly showing their interrelation, naturally orders the bending dynamics according to the characteristic decay rate of its modes, and displays coupling among bending modes in a general flow. This hierarchy naturally yields a low dimensional stochastic dynamical system which recovers and extends previous numerical results and which leads to a fast and efficient numerical method for studying the stochastic nonlinear dynamics of semiflexible polymers in general flows. This formulation will be useful for studying other physical systems described by constrained stochastic partial differential equations.

PACS numbers: 87.15-v,87.15.Aa,83.10.83.50.Ax,83.80.Rs,05.10-a,47.50.+d

In fields such as complex fluids and single-molecule biophysics, one is often interested in dynamic and statistical properties of conformations of *semiflexible biopolymers*, those for which resistance to bending is comparable to or larger than thermal forcing. These polymers may be considered as “wrinkled” rods, in contrast with flexible polymers whose coiled configurations are modeled as diffusive random walks in space [1]. Examples of the two extremes are microtubules, responsible (among other roles) for separating chromosomes during cell division, and long strands of DNA, e.g., those used in the flow experiments of Chu and coworkers [2]

Numerical models of semiflexible polymers often rely on the bead-spring or bead-rod [3, 4, 5] discretizations of the wormlike chain model. Such discretization schemes were originally developed for modeling fully flexible polymers as hundreds of statistically independent extensible or inextensible links [6, 7, 8, 9]. Modeling becomes progressively more complicated as the segments are treated as rods, because the inextensibility constraint must be enforced by tensions which are determined by an algebraic (involving no time derivatives) constraint which couples the motion of all the parts of the chain. Introducing inextensibility presents two additional challenges: multiplicative coupling of the ten-

sion and the configuration of the polymer [10, 11], which leads to *multiplicative* noise in the polymer equation of motion [9]; and a subtle correlation between the configuration of the links which comes from projecting out the momenta degrees of freedom of a system which is constrained to live on a non-Euclidian subspace [6, 12, 13, 14]. Both challenges can be met by using appropriate simulation algorithms [9]—e.g., a mid-step algorithm [6, 7, 13], or an appropriate predictor-corrector algorithm [8]—and by introducing appropriate “metric” forces into the equations of motion [6, 12, 14] and computing them with efficient procedures [4]. Introducing a bending energy in the model yields further complications because inextensibility couples the longitudinal and transversal chain dynamics. The relaxation time of a bending mode of wavenumber j is $\tau_j \equiv \zeta_{\perp} L^4 / (k_j^4 \kappa)$ [15], whereas the longest relaxation time of a rodlike chain is $\tau_{\text{rot}} \equiv \zeta_{\perp} L^3 / (72k_B T)$. Here $\zeta_{\perp} \approx 4\pi\mu / \ln(L/\rho)$ is the perpendicular friction coefficient, L is the chain length, ρ is the chain diameter, μ is the liquid viscosity, $k_j \approx (2j+1)\pi$ is the dimensionless relaxation rate of the j -th bending eigenmode, κ is the chain bending stiffness, k_B is Boltzmann’s constant, and T is temperature. In simulations, the fast shape fluctuations of the chain must be resolved to sample correctly the Boltzmann distribution; therefore, the simulation timestep must

be roughly $\Delta_t \approx 0.1\zeta_{\perp}L^4/((2N+1)^4\pi^4\kappa)$, where N is the shortest wavenumber that can be captured by the discretized model and coincides with the number of rods (minus one) in a bead-rod model. Simulating the terminal relaxation of a chain while resolving the fast modes requires $\approx \tau_{\text{rot}}/\Delta_t$ timesteps, i.e., $\approx 10(2N+1)^4\pi^4L_p/(72L)$, where $L_p \equiv \kappa/k_B T$ is the persistence length of the chain [16]. For the calculation of linear viscoelastic properties, such a hurdle was overcome by simulating the short-time behavior of semiflexible molecules with finely discretized chains, and collapsing the results with those obtained by simulating the long-time behavior with coarsely-discretized chains [3, 5]. Such strategy, however, does not work when applied to nonlinear viscoelastic properties and general flows and deformations, because semiflexible chains buckle when subjected to strong velocity gradients [17]; thus, in nonlinear simulations one has to retain the fine discretization (in order to resolve curvature during buckling) while also simulating long timescales (in order to capture the steady rheological behavior). Therefore, a new, effective method is needed for studying flows of stiff chains at finite temperature.

As in earlier studies, the starting point is the equation of motion for a continuous curve of position $\mathbf{r}(s, t)$ as a function of arclength s and time t , of bending stiffness κ , with inextensibility enforced by a tension Λ , moving in a viscous liquid at temperature T and velocity $\mathbf{U} \approx \mathbf{r} \cdot \nabla \mathbf{U} = \dot{\boldsymbol{\gamma}} \mathbf{r}$ [18, 19]:

$$\partial_t \mathbf{r} - \dot{\boldsymbol{\gamma}} \mathbf{r} = \mathcal{P} (\partial_s \mathbf{F}_{\text{elastic}} + \partial_s \mathbf{F}_{\text{tension}} + \boldsymbol{\xi}) \quad (1)$$

where $\langle \boldsymbol{\xi}(s, t) \boldsymbol{\xi}(s', t') \rangle = 2k_B T \mathcal{P}^{-1} \delta(t-t') \delta(s-s')$, $\mathbf{F}_{\text{elastic}} = -\kappa \partial_s^3 \mathbf{r}$, $\mathbf{F}_{\text{tension}} = \Lambda \partial_s \mathbf{r}$, and the tension Λ is determined by satisfying the inextensibility constraint $|\partial_s \mathbf{r}| = 1$. The mobility tensor $\mathcal{P} \equiv c_{\perp} \hat{\mathbf{n}} \hat{\mathbf{n}} + c_{\parallel} \hat{\mathbf{t}} \hat{\mathbf{t}}$ enforces the anisotropy associated with slender bodies in Stokes flow ($c_{\perp} \equiv 1/\zeta_{\perp}$ and $c_{\parallel} \equiv 2c_{\perp}$ for a slender cylinder). Unlike in previous studies, we work with the Eq. 1 rather than discretizing it into a bead-rod formulation. We pose the dynamic in two dimensions, separating bending from tumbling without constraining the position or orientation of the rod whose configuration is the base state of our perturbation. Differentiating Eq. 1 and recasting the results in terms of tangent and normal vectors $\hat{\mathbf{t}} \equiv \partial_s \mathbf{r} = (\cos \vartheta, \sin \vartheta)$, $\hat{\mathbf{n}} \equiv (-\sin \vartheta, \cos \vartheta)$, yields

$$\vartheta_t \hat{\mathbf{n}} - \dot{\boldsymbol{\gamma}} \hat{\mathbf{t}} = \partial_s \mathcal{P} (\partial_s \mathbf{F}_{\text{elastic}} + \partial_s \mathbf{F}_{\text{tension}} + \boldsymbol{\xi}).$$

Functionally differentiating the elastic energy $E = (\kappa/2) \int_0^L ds (\partial_s \vartheta)^2$ yields the elastic force; whereas

the orientation ϑ does not appear in the energy, the curvature $\partial_s \vartheta$ is suppressed; this introduces a natural perturbation parameter $\varepsilon^2 \equiv k_B T L / \kappa \equiv L / L_p$. Neglecting terms nonlinear in the curvature ϑ_s or its derivatives,

$$\vartheta_t \approx \hat{\mathbf{n}} \dot{\boldsymbol{\gamma}} \hat{\mathbf{t}}(\vartheta) - c_{\perp} \kappa \partial_s^4 \vartheta + \dots \quad (2)$$

suggests representing ϑ as a combination of eigenfunctions of the leading order operator: $L^4 \partial_s^4 \mathcal{W}^{\alpha} = k_{\alpha}^4 \mathcal{W}^{\alpha}$. These biharmonic eigenfunctions generalize many properties of Fourier modes and, for high mode number, asymptote to the Fourier basis [11, 15, 20]. However, they satisfy the boundary conditions (no traction and no torque) imposed on the ends of an elastic rod immersed in a viscous fluid: $\partial_s \mathcal{W}^{\alpha} = \partial_s^2 \mathcal{W}^{\alpha} = 0$. The only allowed 0-mode is independent of s . In this way, the biharmonic eigenfunction basis naturally yields the representation

$$\vartheta(t, s) \equiv \vartheta_0(t) \mathcal{W}^0(s) + \vartheta_{\alpha}(t) \mathcal{W}^{\alpha}(s) \equiv \vartheta_0 + \vartheta_{\alpha} \mathcal{W}^{\alpha}$$

where $\vartheta_0(t)$ is the rod or tumbling term and the $\vartheta_{\alpha}(t)$ are a dynamically ordered sequence of bending terms (summation implied). Adjoint to the set of shape functions is a set of weight eigenfunctions \mathcal{W}_{α} of conjugate boundary conditions $\mathcal{W}_{\alpha} = \partial_s^3 \mathcal{W}_{\alpha} = 0$. The $\{\mathcal{W}^{\alpha}, \mathcal{W}_{\alpha}\}$ are biorthogonal $\int ds \mathcal{W}_{\alpha} \mathcal{W}^{\beta} = L \delta_{\alpha}^{\beta}$, a crucial observation for equipartition of energy,

$$\frac{E}{k_B T} = \frac{1}{2} \varepsilon^{-2} \sum k_{\alpha}^2 \vartheta_{\alpha}^2 \quad (3)$$

which yields immediately the equilibrium variance of any mode $\langle \vartheta_{\alpha}^2 \rangle = (\varepsilon/k_{\alpha})^2$. This representation offers a natural way of capturing the long wavelength bending modes with accuracy while suppressing the short-wavelength modes (which are unimportant in hydrodynamics) by truncating at a small α . The adjoint functions form a natural basis for the tension, which obeys $\Lambda = 0$ at edges: $\Lambda \equiv \Lambda^{\alpha} \mathcal{W}_{\alpha}$

The dynamics of the modes and the constraint can be derived in simple shear ($\dot{\boldsymbol{\gamma}} = \dot{\boldsymbol{\gamma}} \hat{\mathbf{x}} \hat{\mathbf{y}}^T$) by the Galerkin method by multiplying Eq. 1 by the appropriate weight functions (\mathcal{W}_{α} for the modes, \mathcal{W}^{α} for the tensions), integrating along the chain contour, taking the limit for small ε , and dropping terms $\mathcal{O}(\varepsilon^2)$ from the Λ equation and $\mathcal{O}(\varepsilon^3)$ from the ϑ equation,

$$\begin{aligned} 0 &= -c_{\parallel} k_{\beta}^2 \Lambda^{\beta} + [\hat{\mathbf{t}} \dot{\boldsymbol{\gamma}} \hat{\mathbf{n}}]_{\beta} + [\eta^{\parallel}]_{\beta} \quad (4) \\ \dot{\vartheta}_0 &= -\dot{\boldsymbol{\gamma}} (\sin^2 \vartheta_0 + \cos(2\vartheta_0) [\vartheta^2]_0) + \vartheta_{\alpha} \Lambda^{\gamma} \Xi_{0\gamma}^{\alpha} + [\eta^{\perp}]_0 \\ \dot{\vartheta}_{\beta} &= [\hat{\mathbf{n}} \dot{\boldsymbol{\gamma}} \hat{\mathbf{n}}]_{\beta} - \frac{c_{\perp} \kappa}{L^4} k_{\beta}^4 \vartheta_{\beta} + \vartheta_{\alpha} \Lambda^{\gamma} \Xi_{\beta\gamma}^{\alpha} + [\eta_{\perp}]_{\beta} \end{aligned}$$

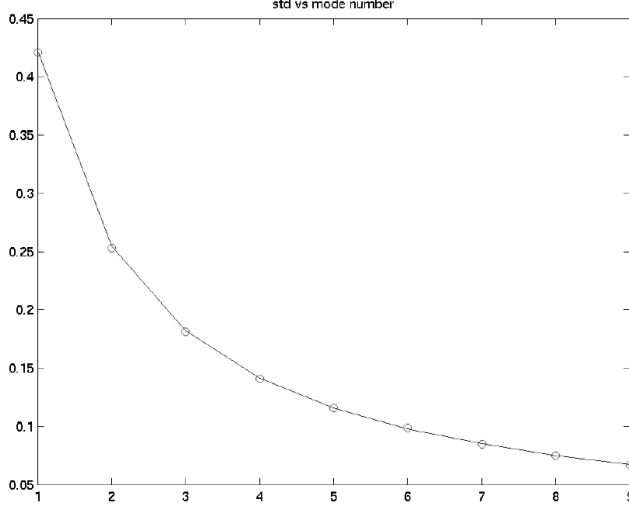


FIG. 1: Theoretical curve ($\sqrt{k_B T L / (\kappa k^2)}$, Eq. 3) and computed values of $\sqrt{\langle \vartheta_\alpha^2 \rangle}$, first 9 bending modes.

where summation over α, γ is implied, $\eta^{\{\parallel, \perp\}} = \{\hat{\mathbf{t}}, \hat{\mathbf{n}}\} \cdot \partial_s \boldsymbol{\xi}$, projection onto the β mode is indicated by $[\dots]_\beta$, and Ξ is an overlap integral of the basis functions which depends on the mobility constants $\{c_\parallel, c_\perp\}$. For isotropic drag, for example, $\Xi_{\beta\gamma}^\alpha \propto \int ds \mathcal{W}^\gamma (k_\beta^2 \mathcal{W}^\beta \mathcal{W}_\alpha - k_\alpha^2 \mathcal{W}^\alpha \mathcal{W}_\beta)$.

Stability – Shear-induced buckling, in which shear and elasticity compete to determine the stability of a non-Brownian rod at fixed ϑ_0 , has been studied analytically, experimentally [21], and numerically [22]. The numerical results show that in simple shear the instability occurs when $(\dot{\gamma}_* L^4 \sin 2\vartheta_0) / (c_\parallel \kappa) = -153.2$. We derive analytically this criterion by expanding the shear terms

$$\gamma_\perp(\vartheta) \equiv \hat{\mathbf{n}} \dot{\gamma} \hat{\mathbf{n}} \approx \gamma_\perp(\vartheta_0) + \vartheta_\alpha \mathcal{W}^\alpha \gamma'_\perp(\vartheta_0) \quad (5)$$

($+\mathcal{O}(\vartheta^2)$)—in simple shear $\gamma_\perp(\vartheta_0) \propto -\sin^2 \vartheta_0$. Expanding the equation of motion and dropping ϑ - and T -dependent terms from the tension, the linear instability criterion is

$$0 = \left(\dot{\gamma}_* \sin 2\vartheta_0 - \frac{c_\perp \kappa}{L^4} k_\beta^4 \right) \vartheta_\beta + \frac{\dot{\gamma}_*}{6} \Xi_{\beta 0}^\alpha \vartheta_\alpha \quad (6)$$

The overlap integral $\Xi_{\beta 0}^\alpha$ is well-approximated by its diagonal contribution $\Xi_{\beta 0}^\beta \delta_\beta^\alpha$. Using the large- α Fourier approximation of the basis functions yields the instability criterion $\dot{\gamma}_* L^4 \sin 2\vartheta_0 / (c_\parallel \kappa) = -162\pi^4 / (76 + 3\pi^2) = -149.4$, with an error of 2.6%. Calculating the diagonal overlap integral reduces the error to .2% [23].

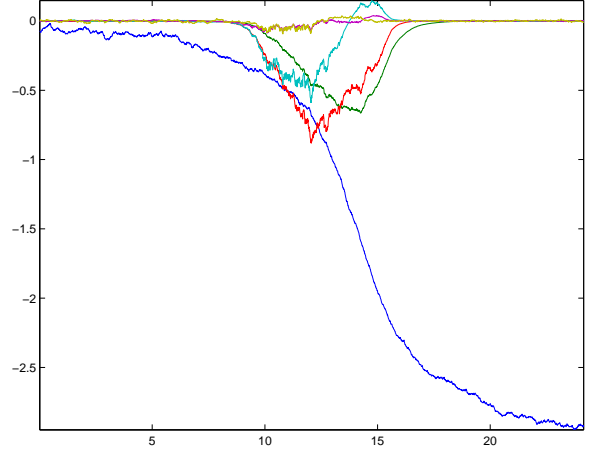


FIG. 2: Stochastic spectral dynamics of bending and tumbling. The curve which leaves the origin traces $\vartheta_0(t)$. The remaining curves describe the bending modes $\vartheta_\alpha(t)$. Each successive mode is smaller in autocorrelation, as expected from the equipartition (Eq. 3). Here $\dot{\gamma} = 8.5 \cdot 10^3 \kappa L^4 / (c_\perp)$, $L = L_p$, and the x-axis is $t\dot{\gamma}$.

Finite temperature – In shear flow, the zero-temperature dynamics asymptote to a straight rod aligned in the velocity direction, because the equation of change of ϑ_0 reduces to $\dot{\vartheta}_0 = -\dot{\gamma} \sin^2 \vartheta_0 \rightarrow 0$ as $\vartheta_0 \rightarrow j\pi$. In the presence of stochastic forces, the dynamics is richer because the $\vartheta_0 = 0$ solution is nonlinearly unstable; thus, the stochastic forces episodically drive ϑ_0 to initiate tumbling events, assisted by shear-induced buckling en route. To study the fully-nonlinear stochastic dynamics we use a midstep algorithm, consistent with variable diffusivity and Stratonovich-interpreted noise [24, 25]. In the absence of shear, the algorithm yields the correct Boltzmann distribution of bending modes (Fig. 1). Illustrative dynamics in the presence of shear are shown in Figs. 2 and 3.

Extensions and connections – One motivation for this work is better understanding of complex fluids. In dilute suspensions, the contribution of molecules to the stress tensor can be calculated via the continuous generalization for wormlike chains [26] of the Kirkwood formula [27]. Quantitative comparison between the efficient spectral numerics and calculations of the stress and molecular conformation (e.g., gyration tensor) by established but inefficient large-scale simulations of bead-rod chains is in progress [17]. Albeit restricted to two dimensions, the fully nonlinear stochastic method is completely general with respect to time-dependent flows and kinematics (shear, extensional, mixed); thus, it will be useful for

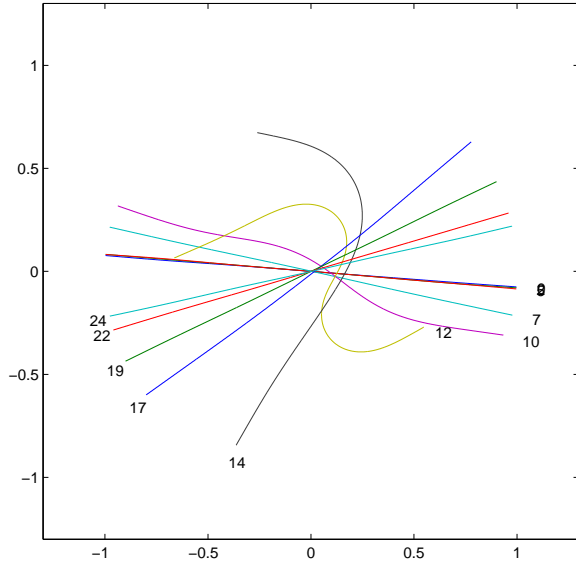


FIG. 3: The same dynamics, represented in real space and imaged at several representative values of $t\dot{\gamma}$. The complex motion is captured by only 6 degrees of freedom.

comparison with “single-bead rheology” studies in actin gels [28]. An extension of the spectral method to include the full three-dimensional representation of semiflexible chains in general flows is underway.

An additional topic for future work is the application of stochastic mode-elimination [29, 30, 31, 32], integrating out the fastest bending modes. Mode elimination renormalizes the noise statistics, and can be used to yield a low-dimensional partial differential equation for the probability density. Because the properties of interest for biopolymers (e.g., configurational changes connected with macroscopic rheology) evolve on slow timescales, stochastic mode elimination is an excellent candidate for mathematically sound yet experimentally relevant analysis. Such a foray would be quite daunting without simple, low dimensional stochastic dynamical systems as in Eq. 4 for which the mapping from Langevin descriptions of trajectories to Fokker-Planck descriptions of probabilities is well-developed.

Acknowledgments – We thank David Morse, Jonathan Mattingly, and Guillaume Bal for useful discussions. Partial financial support was provided by NSF under grant CTS-CAREER-0134389.

-
- [1] M. Doi and S. F. Edwards, *The Theory of Polymer Dynamics* (Oxford University Press, Oxford, 1986).
 - [2] D. Smith, H. Babcock, and S. Chu, *Science* **283**, 1724 (1999).
 - [3] R. Everaers, F. Julicher, A. Ajdari, and A. C. Maggs, *Phys. Rev. Lett.* **82**, 3717 (1999).
 - [4] M. Pasquali and D. C. Morse, *J. Chem. Phys.* **116**, 1834 (2002).
 - [5] M. Pasquali, V. Shankar, and D. C. Morse, *Phys. Rev. E* **64** (2001), paper 020802(R).
 - [6] M. Fixman, *J. Chem. Phys.* **69**, 1527 (1978).
 - [7] P. Grassia and E. J. Hinch, *J. Fluid Mech.* **308**, 255 (1996).
 - [8] T. W. Liu, *J. Chem. Phys.* **90**, 5826 (1989).
 - [9] H. C. Öttinger, *Stochastic Processes in Polymeric Fluids* (Springer Verlag, Berlin, 1996).
 - [10] R. Goldstein and S. Langer, *Phys. Rev. Lett.* **75**, 1094 (1995).
 - [11] R. Goldstein, T. Powers, and C. H. Wiggins, *Phys. Rev. Lett.* **80**, 5232 (1998).
 - [12] D. C. Morse, *Adv. Polymer Sci.* (2003), submitted.
 - [13] E. J. Hinch, *J. Fluid Mech.* **271**, 219 (1994).
 - [14] M. Fixman, *Proc. Nat. Acad. Sci. USA* **74**, 3050 (1974).
 - [15] V. Shankar, M. Pasquali, and D. C. Morse, *J. Rheol.* **46**, 1111 (2002).
 - [16] For a *single* chain of 65 beads (64 rods) and $L_p/L = 10$, this would require $\approx 3.5 \times 10^{10}$ time steps, i.e. approximately one week of computing time on a IBM Power4 processor running at 1.4 GHz.
 - [17] A. Montesi, C. H. Wiggins, and M. Pasquali (2003), in preparation.
 - [18] J. Keller and S. Rubinow, *J. Fluid Mech* **75**, 705 (1976).
 - [19] G. K. Batchelor, *J. Fluid Mech* **41**, 545 (1970).
 - [20] L. D. Landau and E. Lifshitz, *Theory of Elasticity (Theoretical Physics Vol 7)* (Butterworth-Heinemann, New York, 1995).
 - [21] O. L. Forgacs and S. G. Mason, *J. Colloid Interface Sci.* **14** (1958).
 - [22] L. Becker and M. Shelley, *Phys. Rev. Lett.* **87** (2001).
 - [23] The biharmonic eigenfunction basis together with the diagonal approximation of the overlap integrals yield excellent approximation of the bifurcations, (less than 4% error for the first 30 bifurcations).
 - [24] P. Kloeden and E. Platen, *Numerical Solution of Stochastic Differential Equations* (Springer, New York, 1992).
 - [25] We remove stiffness as in [33] and also speed-up the numerics by Taylor-expanding the shear terms and thus storing the overlap integrals (otherwise integrals such as $\int ds W_\beta \sin^2 \vartheta(s)$ must be recomputed at each iteration).
 - [26] D. C. Morse, *Macromolecules* **31**, 7030 (1998).
 - [27] J. Kirkwood, *Macromolecules* (Gordon and Breach, New York, USA).
 - [28] F. Gittes and F. MacKintosh, *Phys Rev E* **58**, 1241 (1998).

- [29] A. Majda, I. Timofeyev, and E. Vanden-Eijnden, Proc. Nat. Acad. Sci. USA **96**, 14687 (1999).
- [30] A. J. Majda, I. Timofeyev, and E. Vanden-Eijnden, Comm. Pure App. Math **54**, 891 (2001).
- [31] T. G. Kurtz, J. Functional Analysis **12**, 55 (1973).
- [32] G. C. Papanicolaou, Rocky Mountain J. Math **6**, 653 (1976).
- [33] T. Hou, J. Lowengrub, and M. Shelley, J. Comp. Phys. **114**, 312 (1994).